arXiv:0811.1344v3 [cond-mat.supr-con] 23 Jan 2009

Thermodynamics of ferromagnetic superconductors with spin-triplet electron pairing

Diana V. Shopova and Dimo I. Uzunov[1]*
CP Laboratory, Institute of Solid State Physics, Bulgarian Academy of Sciences, BG-1784 Sofia, Bulgaria, and
[1] *Department of Physics and Astronomy, University of Western Ontario, London, Ontario N6A 3K7, Canada.*
(Dated: January 23, 2009)

We present a general thermodynamic theory that describes phases and phase transitions of ferromagnetic superconductors with spin-triplet electron Cooper pairing. The theory is based on extended Ginzburg-Landau expansion in powers of superconducting and ferromagnetic order parameters. We propose a simple form for the dependence of theory parameters on the pressure that allows correct theoretical outline of the temperature-pressure phase diagram for which at low temperatures a stable phase of coexistence of p-wave superconductivity and itinerant ferromagnetism appears. We demonstrate that the theory is in an agreement with the experimental data for some intermetallic compounds that are experimentally proven to be itinerant ferromagnetic exhibiting spin-triplet superconductivity. Some basic features of quantum phase transitions in such systems are explained and clarified. We propose to group the spin-triplet ferromagnetic superconductors in two different types of thermodynamic behavior, on the basis of quantitative criterion deduced from the present theory and the analysis of experimental data.

PACS numbers: 74.20.De, 74.25.Dw, 64.70.Tg

I. INTRODUCTION

The spin-triplet or p-wave pairing allows parallel spin orientation of the fermion Cooper pairs in superfluid ^{3}He and unconventional superconductors [1]. For this reason the resulting unconventional superconductivity is robust with respect to effects of external magnetic field and spontaneous ferromagnetic order, so it may coexist with the latter. This general argument implies that there could be metallic compounds and alloys, for which the coexistence of spin-triplet superconductivity and ferromagnetism may be observed.

Particularly, both superconductivity and itinerant ferromagnetic orders can be created by the same band electrons in the metal, which means that spin-1 electron Cooper pairs participate in the formation of the itinerant ferromagnetic order. Moreover, under certain conditions the superconductivity is enhanced rather than depressed by the uniform ferromagnetic order that can generate it, even in cases when the superconductivity does not appear in a pure form as a net result of indirect electron-electron coupling.

The coexistence of superconductivity and ferromagnetism as a result of collective behavior of f-band electrons has been found experimentally for some Uranium-based intermetallic compounds as, UGe_2 [2, 3, 4, 5], URhGe [6, 7, 8], UCoGe [9, 10], and UIr [11, 12]. At low temperature ($T \sim 1$ K) all these compounds exhibit thermodynamically stable phase of coexistence of spin-triplet superconductivity and itinerant (f-band) electron ferromagnetism (in short, FS phase). In UGe_2 and UIr the FS phase appears at high pressure ($P \sim 1$ GPa) whereas in URhGe and UCoGe, the coexistence phase persists up to ambient pressure ($10^5\text{Pa} \equiv 1\text{bar}$).

Experiments, carried out in $ZrZn_2$ [13], also indicated the appearance of FS phase at $T < 1$ K in a wide range of pressures ($0 < P \sim 21$ kbar). In Zr-based compounds the ferromagnetism and the p-wave superconductivity occur as a result of the collective behavior of the d-band electrons. Later experimental results [14, 15] had imposed the conclusion that bulk superconductivity is lacking in $ZrZn_2$, but the occurrence of a surface FS phase at surfaces with higher Zr content than that in $ZrZn_2$ has been reliably demonstrated. Thus the problem for the coexistence of bulk superconductivity with ferromagnetism in $ZrZn_2$ is still unresolved. This raises the question whether the FS phase in $ZrZn_2$ should be studied by surface thermodynamics methods, or it can be investigated by considering that bulk and surface thermodynamic phenomena can be treated on the same footing. Taking in account the mentioned experimental results for $ZrZn_2$ and their interpretation by the experimentalists [13, 14, 15] we assume that the unified thermodynamic approach can be applied, although some specific properties of the FS phase in $ZrZn_2$, if its surface nature is confirmed, will certainly need special study by surface thermodynamics.

Here we will investigate the itinerant ferromagnetism and superconductivity of U- and Zr-based intermetallic compounds within the same general thermodynamic approach. Arguments supporting our point of view are given in several preceding investigations. We should mention that the spin-triplet superconductivity occurs not only in bulk materials, but also in quasi-two-dimensional (2D) systems - thin films and surfaces and quasi-1D wires (see, e.g., Refs. [16]). In $ZrZn_2$ both ferromagnetic and superconducting orders vanish at the same critical pressure P_c, a fact implying that the respective order parameter fields strongly depend on each other and should be studied on the same thermodynamic basis [17].

---

*Corresponding author. Electronic address: d.i.uzunov@gmail.com

The general thermodynamic treatment does not necessarily specify the system spatial dimensionality D: $D = 3$ describes the bulk properties, and $D = 2$ – very thin films and mono-atomic layers. Within Landau theory of phase transitions (see, e.g., Ref. [18]), the system dimensionality can be distinguished by the values of the Landau parameters. Here we specify the values of these parameters from the experimental data for spin-triplet ferromagnetic superconductors. When the Landau parameters are obtained from microscopic theories, their values depend on the dimension D, only if the respective theory takes into account relevant fluctuation modes of order parameter fields, including long-scale fluctuation modes. We are not aware of well developed theories of this type which may figure out the complex behavior of the mentioned systems. Even in simple theories of band electron magnetism, the Landau parameters are very complex functions of the density of states at the Fermi level and related microscopic parameters. Such complexity does not allow direct comparison between the results from microscopic theory and the experimental data. To make a progress in this situation we assume that the material parameters of our theory are loosely defined and may have values, corresponding to various approximate microscopic theories, as mean-field approximation, spin-fluctuation theory, etc.

For all compounds, cited above, the FS phase occurs only in the ferromagnetic phase domain of the $T-P$ diagram. Particularly at equilibrium, and for given P, the temperature $T_F(P)$ of the normal-to-ferromagnetic phase (or N-FM) transition is never lower than the temperature $T_{FS}(P)$ of the ferromagnetic-to-FS phase transition (FM-FS transition). This confirms the point of view that the superconductivity in these compounds is triggered by the spontaneous magnetization $\boldsymbol{M}$, in analogy with the well-known triggering of the superfluid phase A_1 in ^{3}He at mK temperatures by the external magnetic field $\boldsymbol{H}$. Such "helium analogy" has been used in some theoretical studies (see, e.g., Ref. [19, 20]), where Ginzburg-Landau (GL) free energy terms, describing the FS phase were derived by symmetry group arguments. The non-unitary state, with a non-zero value of the Cooper pair magnetic moment, known from the theory of unconventional superconductors and superfluidity in ^{3}He [1], has been suggested firstly in Ref. [19], and later confirmed in other studies [7, 20]; recently, the same topic was comprehensively discussed in [21].

For the spin-triplet ferromagnetic superconductors the trigger mechanism was recently examined in detail [22, 23]. The system main properties are specified by the term in the GL expansion of form $\boldsymbol{M}|\boldsymbol{\psi}|^2$, which represents the interaction of $\boldsymbol{M} = \{M_j; j = 1, 2, 3\}$ with the complex superconducting vector field $\boldsymbol{\psi} = \{\psi_j\}$. Particularly, this term is responsible for the appearance of $\boldsymbol{\psi} \neq 0$ for certain T and P values. A similar trigger mechanism is familiar in the context of improper ferroelectrics [24].

A crucial feature of these systems is the nonzero magnetic moment of the spin-triplet Cooper pairs. As mentioned above, the microscopic theory of magnetism and superconductivity in non-Fermi liquids of strongly interacting heavy electrons (f and d band electrons) is either too complex or insufficiently developed to describe the complicated behavior in itinerant ferromagnetic compounds. Several authors (see [19, 20, 21, 22]) have explored the phenomenological description by a self-consistent mean field theory, and we will essentially use the thermodynamic results, in particular, the analysis in Refs. [22, 23]. Mean-field microscopic theory of spin-mediated pairing leading to the mentioned non-unitary superconductivity state has been developed in Ref. [17] that is in conformity with the phenomenological description that we have done.

In this paper, we present general thermodynamic treatment of systems with itinerant ferromagnetic order and superconductivity due to spin-triplet Cooper pairing of the same band electrons, which are responsible for the spontaneous magnetic moment. We outline their $T-P$ phase diagrams and demonstrate two contrasting types of thermodynamic behavior. The present phenomenological approach includes both mean-field and spin-fluctuation theory (SFT), as the arguments in Ref. [25]. We propose a simple, yet comprehensive, modelling of P dependence of the free energy parameters, resulting in a very good compliance of our theoretical predictions for the shape the $T-P$ phase diagrams with the experimental data (for some preliminary results, see Ref. [26].

The theoretical analysis is done by the standard methods of phase transition theory [18]. Treatment of fluctuation effects and quantum correlations [18, 27] is not included in this study. But the parameters of the generalized GL free energy may be considered either in mean-field approximation as here, or as phenomenologically renormalized parameters which are affected by additional physical phenomena, as for example, spin fluctuations.

We demonstrate with the help of present theory that we can outline different possible topologies for the $T-P$ phase diagram, depending on the values of Landau parameters, derived from the existing experimental data. We show that for unconventional (spin-triplet) ferromagnetic superconductors (FSs) there exist two distinct types of behavior, which we denote as Zr-type (or, alternatively, type I) and U-type (or, type II). This classification of the FS, first mentioned in Ref. [26], is based on the reliable interrelationship between a quantitative criterion derived by us and the thermodynamic properties of the spin-triplet FSs (see Sec. III.C and Sec. IV.D). Our approach can be also applied to URhGe, UCoGe, and UIr. Our results shed light on the problems connected with the order of the quantum phase transitions at ultra-low and zero temperatures. They also raise the question for further experimental investigations of the detailed structure of the phase diagrams in the high-P/low-T region.

In Sec. II we present the GL free energy of ferromagnetic superconductors with spin-triplet Cooper pairing. Here the arguments for the proposed simple pressure dependence of the Landau parameters are explained and, as the comparison with experimental data demonstrates, the chosen P-dependence gives quite satisfactory quantitative results. In more detailed studies one may use more complex pressure dependence of material parameters. In Sec. III we present our theoretical results for the various possible shapes of the phase diagram, multi-critical points, quantum phase transitions. The theory predicts all types of phase transition points and lines which are needed in the description of real itinerant ferromagnets with spin-triplet Cooper pairing. In Sec. IV we compare our theoretical results with the experimental data for some intermetallic compounds. The comparison gives very good quantitative agreement between experiment and theory for all known experimental examples, except URhGe, where a particular form of pressure dependence of the material parameters should be suggested. On the basis of this analysis we propose a possible classification of unconventional ferromagnetic superconductors, showing on the basis of quantitative criterion that they are of two types (Sec. IV.E). In Sec. V we summarize our findings and some unresolved problems which are beyond the scope of the present study.

II. GENERALIZED GINZBURG-LANDAU FREE ENERGY

Following Ref. [22], the free energy per unit volume, $F/V = f(\boldsymbol{\psi}, \boldsymbol{M})$, can be written in the form

$$f(\boldsymbol{\psi}, \boldsymbol{M}) = a_s|\boldsymbol{\psi}|^2 + \frac{b_s}{2}|\boldsymbol{\psi}|^4 + \frac{u_s}{2}|\boldsymbol{\psi}^2|^2 + \frac{v_s}{2}\sum_{j=1}^{3}|\psi_j|^4 + a_f\boldsymbol{M}^2 + \frac{b_f}{2}\boldsymbol{M}^4 + i\gamma_0\boldsymbol{M}\cdot(\boldsymbol{\psi}\times\boldsymbol{\psi}^*) + \delta\boldsymbol{M}^2|\boldsymbol{\psi}|^2. \qquad (1)$$

The material parameters satisfy $b_s > 0$, $b_f > 0$; $a_s = \alpha_s(T - T_s)$, and $a_f = \alpha_f[T^n - T_f^n(P)]$, where $n = 1$ gives the standard form of a_f, and $n = 2$ applies for SFT [25] and the Stoner-Wohlfarth model [28]. The terms proportional to u_s and v_s describe, respectively, the anisotropy of the spin-triplet electron Cooper pairs and the crystal anisotropy. Next, $\gamma_0 \sim J$ (with $J > 0$, the ferromagnetic exchange constant) and $\delta > 0$ are parameters of the $\boldsymbol{\psi}$-$\boldsymbol{M}$ interaction terms. Previous studies [22] have shown that the anisotropy represented by the u_s and v_s terms in Eq. (1), slightly perturbs the size and shape of the stability domains of the phases, while similar effects can be achieved by varying the b_s factor in the $b_s|\boldsymbol{\psi}|^4$ term. For such reasons, in the present analysis we ignore the anisotropy terms, setting $u_s = v_s = 0$, and consider $b_s \equiv b > 0$ as an effective parameter. Then, without loss of generality, we may choose the magnetization vector to have the form $\boldsymbol{M} = (0, 0, M)$.

According to the microscopic theory of band magnetism and superconductivity, the macroscopic material parameters in Eq. (1) depend in a very complex way on the density of states at the Fermi level and related microscopic quantities [29]. That is why we can hardly use the microscopic characteristics of these complex metallic compounds in order to elucidate their thermodynamic properties, in particular, in outlining their phase diagrams in some details. However, some simple microscopic models give useful results, for example, the zero temperature Stoner-type model employed in Ref. [30].

We redefine for convenience the free energy, Eq. (1), in a dimensionless form by $\tilde{f} = f/(b_f M_0^4)$, where $M_0 = [\alpha_f T_{f0}^n/b_f]^{1/2} > 0$ is the value of the magnetization M corresponding to the pure magnetic subsystem ($\boldsymbol{\psi} \equiv 0$) at $T = P = 0$ and $T_{f0} = T_f(0)$. Order parameters assume the scaling $m = M/M_0$ and $\boldsymbol{\varphi} = \boldsymbol{\psi}/[(b_f/b)^{1/4}M_0]$ and in result, the free energy becomes

$$\tilde{f} = r\phi^2 + \frac{\phi^4}{2} + tm^2 + \frac{m^4}{2} + 2\gamma m\phi_1\phi_2\sin\theta + \gamma_1 m^2\phi^2, \quad (2)$$

where $\phi_j = |\varphi_j|$, $(j = 1, 2, 3)$, $\phi = |\boldsymbol{\varphi}|$, and $\theta = (\theta_2 - \theta_1)$ is the phase angle between the complex $\varphi_1 = \phi_1 e^{i\theta_1}$ and $\varphi_2 = \phi_2 e^{\theta_2}$. Note, that the third phase angle, θ_3, corresponding to the third complex field component $\varphi_3 = \phi_3 e^{i\theta_3}$, does not enter explicitly in the free energy density $\tilde{f}$, given by Eq. (2), which is a natural result of the continuous space degeneration. The dimensionless parameters t, r, γ and γ_1 in Eq. (2) are given by

$$t = \tilde{T}^n - \tilde{T}_f^n(P), \quad r = \kappa(\tilde{T} - \tilde{T}_s), \quad (3)$$

where $\kappa = \alpha_s b_f^{1/2}/\alpha_f b^{1/2} T_{f0}^{n-1}$, $\gamma = \gamma_0/[\alpha_f T_{f0}^n b]^{1/2}$, and $\gamma_1 = \delta/(bb_f)^{1/2}$. The reduced temperatures are: $\tilde{T} = T/T_{f0}$, $\tilde{T}_f(P) = T_f(P)/T_{f0}$, and $\tilde{T}_s(P) = T_s(P)/T_{f0}$.

Here we will outline the simple assumptions for the P-dependence of the t, r, γ, and γ_1 parameters in Eq. (2). Particularly, we assume that only T_f has a significant P-dependence, described by

$$\tilde{T}_f(P) = (1 - \tilde{P})^{1/n}, \quad (4)$$

where $\tilde{P} = P/P_0$ and P_0 is a characteristic pressure deduced later. In ZrZn$_2$ and UGe$_2$ the P_0 values are very close to the critical pressure P_c, at which both the ferromagnetic and superconducting orders vanish, but in other systems this is not necessarily the case. As we will discuss, the nonlinearity ($n = 2$) of $T_f(P)$ in $ZrZn_2$ and UGe_2 is relevant at relatively high P, at which the N-FM transition temperature $T_F(P)$ may not coincide with $T_f(P)$. The form (3) of the model function $\tilde{T}_f(P)$ is consistent with preceding experimental and theoretical investigations of the N-FM phase transition in $ZrZn_2$ and UGe_2 (see, e.g., Refs. [4, 20, 31]). Here we consider only non-negative values of the pressure P; for effects at $P < 0$, see, e.g., Ref. [32].

The model function (4) is defined for $P \leq P_0$, in particular, for the case of $n > 1$, but we should have in mind that, in fact, the thermodynamic analysis of Eq. (2) includes the parameter t rather than $T_f(P)$. This parameter is given by

$$t(T, P) = \tilde{T}^n - 1 + \tilde{P}, \tag{5}$$

and is well defined for any $\tilde{P}$. This allows to consider pressures $P > P_0$ within the free energy (2).

The model function $\tilde{T}_f(P)$ can be naturally generalized to $\tilde{T}_f(P) = (1 - \tilde{P}^{\beta})^{1/\alpha}$ but the present needs of interpretation of experimental data do not require this; hereafter we use Eq. (3) which corresponds to $\beta = 1$ and $\alpha = n$). Besides, other analytical forms of $\tilde{T}_f(\tilde{P})$ can also be tested in the free energy (2), in particular, expansion in powers of $\tilde{P}$, or, alternatively, in $(1 - \tilde{P})$ which satisfy the conditions $\tilde{T}_f(0) = 1$ and $\tilde{T}_f(1) = 0$. Note, that in URhGe the slope of $T_F(P) \sim T_f(P)$ is positive from $P = 0$ up to high pressures [8] and for this compound the form (3) of $\tilde{T}_f(P)$ is inconvenient. Here we apply the simplest form for the P-dependence, namely, Eqs. (4) – (5).

III. PHASE TRANSITIONS AND MULTICRITICAL POINTS

A. Phase of coexistence of ferromagnetism and superconductivity

The simplified model (2) is capable of describing the main thermodynamic properties of spin-triplet ferromagnetic superconductors. For $r > 0$, i.e., $T > T_s$, there are three stable phases: (i) the normal (N-) phase, given by $\phi = m = 0$ (stability conditions: $t \geq 0$, $r \geq 0$); (ii) the pure ferromagnetic phase (FM phase), given by $m = (-t)^{1/2} > 0$, $\phi = 0$, which exists for $t < 0$ and is stable, provided $r \geq 0$ and $r \geq (\gamma_1 t + \gamma |t|^{1/2})$, and (iii) the phase of coexistence of ferromagnetic order and superconductivity (FS phase), given by sin$\theta = \mp 1$, $\phi_3 = 0$, $\phi_1 = \phi_2 = \phi/\sqrt{2}$, where

$$\phi^2 = \kappa(\tilde{T}_s - \tilde{T}) \pm \gamma m - \gamma_1 m^2 \geq 0. \tag{6}$$

The magnetization m satisfies the equation

$$c_3 m^3 \pm c_2 m^2 + c_1 m \pm c_0 = 0 \tag{7}$$

with coefficients $c_0 = \gamma\kappa(\tilde{T} - \tilde{T}_s)$,

$$c_1 = 2\left[\tilde{T}^n + \kappa\gamma_1(\tilde{T}_s - \tilde{T}) + \tilde{P} - 1 - \frac{\gamma^2}{2}\right], \tag{8}$$

$$c_2 = 3\gamma\gamma_1, \quad c_3 = 2(1 - \gamma_1^2). \tag{9}$$

The FS phase has two thermodynamically equivalent phase domains that can be distinguished by the upper and lower signs ($\pm$) of some terms in Eqs. (6) and (7). The upper sign describes the domain (labelled bellow again by FS), with $m > 0$, sin$\theta = -1$, whereas the lower sign describes the conjunct domain FS*, where $m < 0$ and sin$\theta = 1$; for details, see, Ref. [22]. Here we consider one of the two thermodynamically equivalent phase domains, namely, the domain FS, which is stable for $m > 0$ (FS* is stable for $m < 0$). In the absence of external symmetry breaking field, such "one-domain approximation" correctly presents the main thermodynamic properties described by the model (1). The FS phase domain, given by upper sign Eqs.(6) and (7), satisfies the stability conditions: $\gamma M \geq 0$ and

$$\kappa(\tilde{T}_s - \tilde{T}) \pm \gamma m - 2\gamma_1 m^2 \geq 0, \tag{10}$$

$$3(1-\gamma_1^2)m^2 + 3\gamma\gamma_1 m + \tilde{T}^n - 1 + \tilde{P} + \kappa\gamma_1(\tilde{T}_s - \tilde{T}) - \frac{\gamma^2}{2} \geq 0. \tag{11}$$

These results are valid for $T_f(P) > T_s(P)$, which excludes any pure superconducting phase ($\boldsymbol{\psi} \neq 0, m = 0$) in accordance with the available experimental data.

For $r < 0$, and $t > 0$ the model (1)-(2) exhibits a stable pure superconducting phase ($\phi_1 = \phi_2 = m = 0$, $\phi_3^2 = -r$) [22]. This phase may occur in the temperature domain $T_f(P) < T < T_s$. For systems, where $T_f(0) \gg T_s$, this is a domain of pressure in a very close vicinity of $P_0 \sim P_c$, where $T_F(P) \sim T_f(P)$ decreases to values lower than T_s. Such a situation is described by the model (2) only if $T_s > 0$. This case is interesting from the experimental point of view only when $T_s > 0$ is big enough to enter in the scope of experimentally measurable temperatures. Up to date a pure superconducting phase has not been observed within the accuracy of experiments on the studied metallic compounds. For this reason, in the reminder of this paper we will assume that the critical temperature T_s of the generic superconducting phase transition is either non-positive ($T_s \leq 0$), or has a small positive value which can be neglected in the analysis of the available experimental data.

The negative values of the critical temperature T_s of the generic superconducting phase transition are generally possible and produce a variety of phase diagram topologies (Sec. III.B). The value of T_s depends on the strength of the interaction, responsible for the formation

TABLE I: Theoretical results for the location [$(\tilde{T},\tilde{P})$-*reduced* coordinates] of the tricritical points $A \equiv (\tilde{T}_A, \tilde{P}_A)$ and $B \equiv (\tilde{T}_B, \tilde{P}_B)$, the critical-end point $C \equiv (\tilde{T}_C, \tilde{P}_C)$, and the point of temperature maximum, $max = (\tilde{T}_m, \tilde{P}_m)$ on the curve $\tilde{T}_{FS}(\tilde{P})$ of the FM-FS phase transitions of first and second order (for details, see Sec. III.B). The first column shows $\tilde{T}_N \equiv \tilde{T}_{(A,B,C,m)}$. The second column stands for $t_N = t_{(A,B,C,m)}$. The reduced pressure values $\tilde{P}_{(A,B,C,m)}$ of points A, B, C, and *max* are denoted by $\tilde{P}_N(n)$: $n = 1$ stands for the linear dependence $T_f(P)$, $n = 2$ - for the nonlinear dependence of $T_f(P)$ and $t(T)$, corresponding to SFT.

N	$\tilde{T}_N$	t_N	$\tilde{P}_N(n)$
A	$\tilde{T}_s$	$\gamma^2/2$	$1 - \tilde{T}_s^n + \gamma^2/2$
B	$\tilde{T}_s + \gamma^2(2+\gamma_1)/4\kappa(1+\gamma_1)^2$	$-\gamma^2/4(1+\gamma_1)^2$	$1 - \tilde{T}_B^n - \gamma^2/4(1+\gamma_1)^2$
C	$\tilde{T}_s + \gamma^2/4\kappa(1+\gamma_1)$	0	$1 - \tilde{T}_C^n$
max	$\tilde{T}_s + \gamma^2/4\kappa\gamma_1$	$-\gamma^2/4\gamma_1^2$	$1 - \tilde{T}_m^n - \gamma^2/4\gamma_1^2$

of the spin-triplet Cooper pairs, which means that the P-dependence of T_s specifies the sensitivity of electron couplings to the crystal lattice properties. This is an effect which might be included in our theoretical scheme by introducing some convenient pressure dependence of T_s. To do so we need information either from experimental data or from a comprehensive microscopic theory.

Usually, $T_s \leq 0$ is interpreted as a lack of any superconductivity, but here the same non-positive values of T_s are effectively enhanced to positive values by the interaction parameter γ which triggers the superconductivity up to superconducting phase transition temperatures $T_{FS}(P) > 0$. This is readily seen from Table 1, where we present the reduced characteristic temperatures on the FM-FS phase transition line $\tilde{T}_{FS}(\tilde{P})$, calculated from the present theory, namely, $\tilde{T}_m$ - the maximum of the curve $\tilde{T}_{FS}(\tilde{P})$ (if available; see Sec. III.B), the temperatures $\tilde{T}_A$ and $\tilde{T}_B$, corresponding to the tricritical points $A \equiv (\tilde{T}_A, \tilde{P}_A)$, $B \equiv (\tilde{T}_B, \tilde{P}_B)$, and the temperature $\tilde{T}_C$ corresponding to the critical-end point $C \equiv (\tilde{T}_C, \tilde{P}_C)$. The theoretical derivation of the dependence of the multi-critical temperatures $\tilde{T}_A$, $\tilde{T}_B$, and $\tilde{T}_C$ on γ, γ_1, κ, and $\tilde{T}_s$, as well as the dependence of $\tilde{T}_m$ on the same model parameters is outlined in Sec. III.B. All these temperatures as well as the whole phase transition line $T_{FS}(P)$ are considerably boosted above T_s owing to positive terms of order γ^2. If $\tilde{T}_s < 0$, the superconductivity appears, provided $\tilde{T}_m > 0$, i.e., when $\gamma^2/4\kappa\gamma_1 > |\tilde{T}_s|$ (see Table 1).

B. Temperature-pressure phase diagram

Although the structure of the FS phase is complicated, some of the results can be obtained in analytical form. A more detailed outline of the phase domains, for example, in $T - P$ phase diagram, can be done by using suitable values of material parameters in the free energy (2): P_0, T_{f0}, T_s, κ, γ, and γ_1. Here we present some of the analytical results for the phase transition lines and the multi-critical points. Typical shapes of phase diagrams derived directly from Eq. (2) are given in Figs.1-6. Fig. 1 shows the phase diagram calculated from Eq. (2) for parameters, corresponding to the experimental data [13] for ZrZn$_2$. Figs. 2-3 show the low-temperature and the high-pressure parts of the same phase diagram (see Sec. IV for details). Figs. 4-6 show the phase diagram calculated for the experimental data [2, 4] of UGe$_2$ (see Sec.IV). In ZrZn$_2$, UGe$_2$, as well as in UCoGe and UIr, critical pressure P_c exists, where both superconductivity and ferromagnetic orders vanish.

As in experiments, we find out from our calculation that in the vicinity of $P_0 \sim P_c$, the FM-FS phase transition is of first order, denoted by the solid line BC in Figs. 2,3,5,6. At lower pressure the same phase transition is of second order, shown by the dotted lines in the same figures. The second order phase transition line $\tilde{T}_{FS}(P)$ separating the FM and FS phases is given by the solution of the equation

$$\tilde{T}_{FS}(\tilde{P}) = \tilde{T}_s + \tilde{\gamma}_1 t_{FS}(\tilde{P}) + \tilde{\gamma}[-t_{FS}(\tilde{P})]^{1/2}, \qquad (12)$$

where $t_{FS}(\tilde{P}) = t(T_{FS}, \tilde{P}) \leq 0$, $\tilde{\gamma} = \gamma/\kappa$, $\tilde{\gamma}_1 = \gamma_1/\kappa$, and $0 < \tilde{P} < \tilde{P}_B$; P_B is the pressure corresponding to the multi-critical point B, where the first-order line $T_{FS}(P)$ terminates, as clearly seen in Figs. 3 and 6. Eq. (12)strictly coincides with the stability condition for the FM-phase with respect to the appearance of FS-phase.

Additional information for the shape of the FM-FS phase transition line can be obtained by the derivative $\tilde{\rho} = \partial\tilde{T}_{FS}(\tilde{P})/\partial\tilde{P}$, namely,

$$\tilde{\rho} = \frac{\tilde{\rho}_s + \tilde{\gamma}_1 - \tilde{\gamma}/2(-t_{FS})^{1/2}}{1 - n\tilde{T}_{FS}^{n-1}\left[\tilde{\gamma}_1 - \tilde{\gamma}/2[(-t_{FS})^{1/2}\right]}, \qquad (13)$$

where $\tilde{\rho}_s = \partial\tilde{T}_s(\tilde{P})/\partial\tilde{P}$. Note, that Eq. (13) is obtained from Eqs. (5) and (12).

The shape of the line $\tilde{T}_{FS}(P)$ can vary depending on the theory parameters (see, e.g., Figs. 2, 5). For certain ratios of $\tilde{\gamma}$, $\tilde{\gamma}_1$, and values of $\tilde{\rho}_s$, the curve $\tilde{T}_{FS}(\tilde{P})$ exhibits a maximum $\tilde{T}_m = \tilde{T}_{FS}(\tilde{P}_m)$, given by the solution of $\tilde{\rho}(\tilde{\rho}_s, T_m, P_m) = 0$. This maximum is clearly seen in Figs. 5, 6. To locate the maximum we need to know $\tilde{\rho}_s$. We have already assumed that T_s does not depend on P, as explained above, which from the physical point of view means that the function $T_s(P)$ is flat enough to

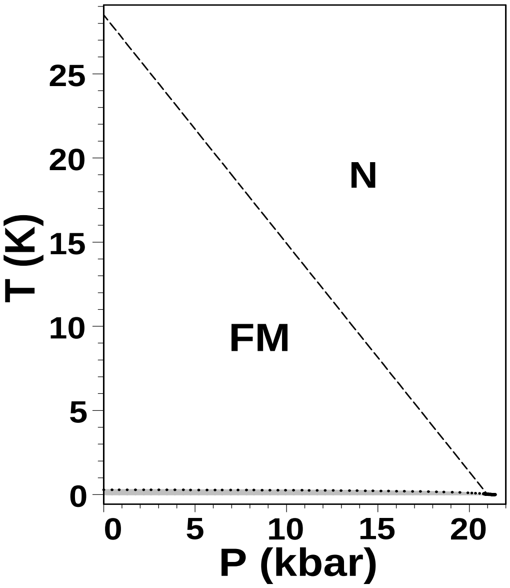

FIG. 1: $T-P$ diagram of ZrZn$_2$ calculated for $T_s=0$, $T_{f0}=28.5$ K, $P_0=21$ kbar, $\kappa=10$, $\tilde{\gamma}=2\tilde{\gamma}_1\approx 0.2$, and $n=1$. The dotted line represents the FM-FS transition and the dashed line stands for the second order N-FM transition. The dotted line has a zero slope at $P=0$. The low-temperature and high-pressure domains of the FS phase are seen more clearly in the following Figs. 2, 3.

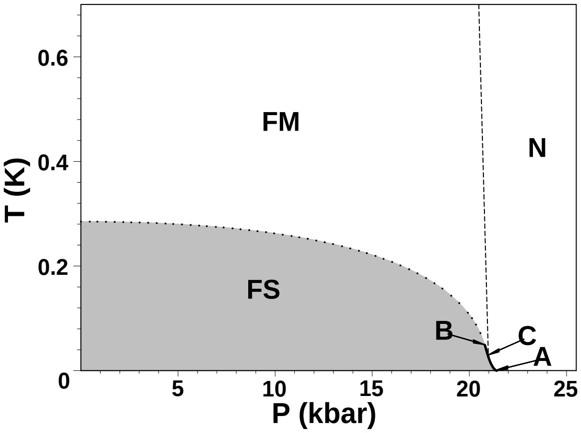

FIG. 2: Details of Fig. 1 with expanded temperature scale. The points A, B, C are located in the high-pressure part ($P\sim P_c\sim 21$ kbar). The *max* point is at $P\approx 0$ kbar. The FS phase domain is shaded. The dotted line shows the second order FM-FS phase transition with $P_m\approx 0$. The solid straight line BC shows the fist-order FM-FS transition for $P>P_B$. The quite flat solid line AC shows the first order N-FS transition (the lines BC and AC are more clearly seen in Fig. 3. The dashed line stands for the second order N-FM transition.

allow the approximation $\tilde{T}_s\approx 0$ without a substantial error in the results. From our choice of P-dependence of the free energy (2)parameters, it follows that $\tilde{\rho}_s=0$.

Setting $\tilde{\rho}_s=\tilde{\rho}=0$ in Eq. (13), we obtain

$$t(T_m,P_m)=-\frac{\tilde{\gamma}^2}{4\tilde{\gamma}_1^2}, \tag{14}$$

namely, the value $t_m(T,P)=t(T_m,P_m)$ at the maximum $T_m(P_m)$ of the curve $T_{FS}(P)$. Substituting t_m back in Eq. (12) we obtain T_m, and with its help we also obtain the pressure P_m, both given in Table 1, respectively.

We want to draw the attention to a particular feature of the present theory that the coordinates T_m and P_m of the maximum (point "*max*") on the curve $T_{FS}(P)$, and also the results of various calculations with the help of Eqs. (12) and (13) are expressed in terms of the reduced interaction parameters $\tilde{\gamma}$ and $\tilde{\gamma}_1$. Thus, using certain experimental data for T_m, P_m, as well as Eqs. (12) and (13) for T_{FS}, T_s and the derivative ρ at particular values of the pressure P, $\tilde{\gamma}$ and $\tilde{\gamma}_1$ can be calculated without any additional information, for example, for the parameter κ. This property of the model (2) is very useful in the practical work with the experimental data.

The conditions for existence of a maximum on the curve $T_{FS}(P)$ can be determined by requiring $\tilde{P}_m>0$ and $\tilde{T}_m>0$ and using the respective formulae for these quantities, shown in Table 1. This *max* always occurs in systems where $T_{FS}(0)\leq 0$ and the low-pressure part of the curve $T_{FS}(P)$ terminates at $T=0$ for some non-negative critical pressure P_{0c} (see Sec. III.C). But the maximum may occur also for some sets of material parameters, when $T_{FS}(0)>0$ (see Fig. 2, where $P_m=0$). All these shapes of the line $T_{FS}(P)$ are described by the model (2). Irrespective of the particular shape, the curve $T_{FS}(P)$ given by Eq. (12) always terminates at the tricritical point (labelled B), with coordinates (P_B,T_B) (see, e.g., Figs. 3, 6).

At pressure $P>P_B$ the FM-FS phase transition is of first order up to the critical-end point C. For $P_B<P<P_C$ the FM-FS phase transition is given by the straight line BC; see, Figs. 3, 6. All three phase transition lines - N-FM, N-FS, and FM-FS - terminate at point C. For $P>P_C$ the FM-FS phase transition occurs on a rather flat, smooth line of equilibrium transition of first order up to a second tricritical point A with $P_A\sim P_0$ and $T_A\sim 0$. Finally, the third transition line terminating at the point C describes the second order phase transition N-FM. The reduced temperatures $\tilde{T}_N$ and pressures $\tilde{P}_N$, $N=$ (A, B, C, *max*) at the three multi-critical points (A, B, C) and the maximum $T_m(P_m)$ are given in Table 1. Note that, for any set of material parameters, $T_A<T_C<T_B<T_m$ and $P_m<P_B<P_C<P_A$.

There are other types of phase diagrams, resulting from the model (2). For negative values of the generic superconducting temperature T_s several other topologies of the $T-P$ diagram can be outlined. The results for the multicritical points, presented in Table 1 show that when T_s lowers below $T=0$, also T_C decrease, firstly to zero, and then to negative values. When $T_C=0$ the direct N-FS phase transition of first order disappears and the point C becomes a very special zero-temperature multicritical point. As seen from Table 1, this happens for $T_s=-\gamma^2T_f(0)/4\kappa(1+\gamma_1)$. The further decrease of T_s

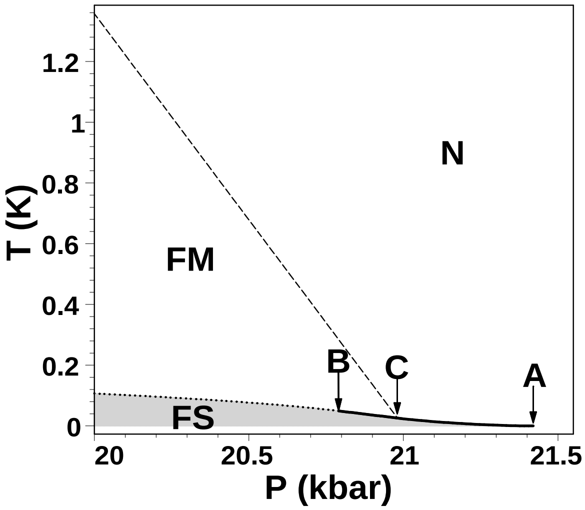

FIG. 3: High-pressure part of the phase diagram of $ZrZn_2$, shown in Fig. 1. The thick solid lines AC and BC show the first-order transitions N-FS, and FM-FS, respectively. Other notations are explained in Figs. 1, 2.

causes the point C to fall below the zero temperature and then the zero-temperature phase transition of first order near P_c splits into two zero-temperature phase transitions: a second order N-FM transition and a first order FM-FS transition, provided T_B still remains positive.

At lower T_s also the point B falls below $T = 0$ and the FM-FS phase transition becomes entirely of second order. For very extreme negative values of T_s, a very large pressure interval below P_c may occur where the FM phase is stable up to $T = 0$. Then the line $T_{FS}(P)$ will exist only for relatively small pressure values ($P \ll P_c$). This shape of the stability domain of the FS phase is also possible in real systems.

C. Quantum phase transitions

The effects of quantum correlations on the phase transition properties at ultra-low and zero temperature, known as quantum phase transitions [27], can also be described by the free energy (1), as mentioned above. The time-dependent quantum fluctuations, which describe the intrinsic quantum dynamics of spin-triplet ferromagnetic superconductors, are not included in the model (1), but some basic properties of the quantum phase transitions can be outlined within the classical limit, namely, by the free energy model (1) – (2).

Generally, both classical (thermal) and quantum fluctuations are investigated by the method of the renormalization group (RG) [18], which is specially intended to treat the generalized action of system, where the order parameter fields fluctuate in time t and space $\vec{x}$ [18, 27]. These effects, which are beyond the scope of the paper, lead either to precise treatment of the narrow critical region in a very close vicinity of second order phase transition lines, or to a fluctuation-driven change of the phase transition order. But, the thermal fluctuation and quantum correlation effects on the thermodynamics of a given system can be unambiguously estimated only after the results from the counterpart simpler theory, where these effects are not present, are known and, hence, the distinction in the thermodynamic properties predicted by the respective variants of the theory can be established. Here we show that the basic low and ultra-low temperature properties of the spin-triplet FSs, as given by the preceding experiments, are derived from the model (1) without any account of fluctuation phenomena and quantum correlations. The latter might be of use in a more detailed consideration of the close vicinity of quantum critical points in the phase diagrams of spin-triplet FSs. Here we show that the theory predicts quantum critical phenomena only for quite particular physical conditions whereas the low- and zero-temperature phase transitions of the first order are favored by both symmetry arguments and detailed thermodynamic analysis.

There is a number of experimental [9, 33] and theoretical [17, 34, 35] studies on the problem of quantum phase transitions in unconventional ferromagnetic superconductors, including the mentioned intermetallic compounds. Some of them are based on different theoretical schemes, and do not refer to the model (1). Other, for example, those in Ref. [34] reported results about the thermal and quantum fluctuations, described by the model (2) before the comprehensive knowledge of the results from the basic treatment, given by the present investigation. In such cases one could not be sure about the correct interpretation of the results from the RG and the possibilities for their application to particular zero temperature phase transitions. Here we present basic results for the zero-temperature phase transitions, described by the model (2).

The RG investigation [34] has demonstrated up to two loop order of the theory that the thermal fluctuations of the order parameter fields re-scale the model (2) in way which corresponds to first order phase transitions in magnetically anisotropic systems. This result is important for the metallic compounds, we consider here, because in all of them magnetic anisotropy is present. The uniaxial magnetic anisotropy in $ZrZn_2$ is much more weak than in UGe_2 but cannot be neglected when fluctuation effects are accounted for. Owing to the particular symmetry of the model (2), for the case of magnetic isotropy (Heisenberg symmetry), the RG study reveals an entirely new class of (classical) critical behavior. Besides, the different spatial dimensions of the superconducting and magnetic quantum fluctuations imply a lack of stable quantum critical behavior even when the system is completely magnetically isotropic. The pointed arguments and preceding results lead to the reliable conclusion that the phase transitions, which have already been proven to be first order in the lowest order approximation, where thermal and quantum fluctuations are neglected, will not undergo a fluctuation-driven change of the phase transition order from first to second. Such picture is described

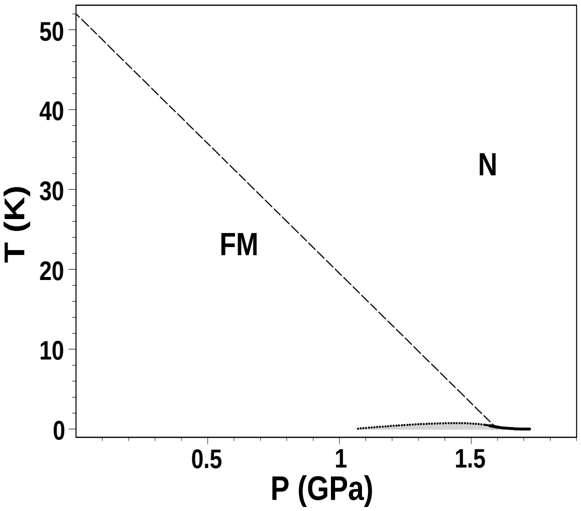

FIG. 4: $T-P$ diagram of UGe$_2$ calculated taking $T_s = 0$, $T_{f0} = 52$ K, $P_0 = 1.6$ GPa, $\kappa = 4$, $\tilde{\gamma} = 0.0984$, $\tilde{\gamma_1} = 0.1678$, and $n = 1$. The dotted line represents the FM-FS transition and the dashed line stands for the N-FM transition. The low-temperature and high-pressure domains of the FS phase are seen more clearly in the following Figs. 5, 6.

below, in Sec. IV, and it corresponds to the behavior of real compounds.

Our results definitely show that the quantum phase transition near P_c is of first order. This is valid for the whole N-FS phase transition below the critical-end point C, as well as the straight line BC. The simultaneous effect of thermal and quantum fluctuations do not change the order of the N-FS transition, and it is unlikely to suppose that thermal fluctuations of the superconductivity field $\boldsymbol{\psi}$ can ensure a fluctuation-driven change of the order of the FM-FS transition along the line BC. Usually, the fluctuations of $\boldsymbol{\psi}$ in low temperature superconductors are small and slightly influence the phase transition in the very narrow critical region in the vicinity of phase transition point. This effect is very weak and can hardly be observed in any experiment on low-temperature superconductors. Besides, the fluctuations of the magnetic induction $\boldsymbol{B}$ always tend to a fluctuation-induced first order phase transition rather than to the opposite effect - the generation of magnetic fluctuations with infinite correlation length at the equilibrium phase transition point and, hence, a second order phase transition [18, 36]. Thus we can reliably conclude that the first order phase transitions at low-temperatures, represented by the lines BC and AC in vicinity of P_c do not change their order as a result of thermal and quantum fluctuations.

Quantum critical behavior for continuous phase transitions in spin-triplet ferromagnetic superconductors with magnetic anisotropy can therefore be observed at other zero-temperature transitions, which may occur in these systems far from the critical pressure P_c. This is possible when $T_{FS}(0) = 0$ and the $T_{FS}(P)$ curve terminates at $T = 0$ at one or two quantum (zero-temperature) critical points: $P_{0c} < P_m$ - "lower critical pressure", and $P'_{0c} > P_m$ – "upper critical pressure." To obtain these critical pressures one should solve Eq. (12) with respect to P, provided $T_{FS}(P) = 0$, $T_m > 0$ and $P_m > 0$, namely, when the continuous function $T_{FS}(P)$ exhibits a maximum. The critical pressure P'_{0c} is bounded in the relatively narrow interval (P_m, P_B) and can appear for some special sets of material parameters (r, t, γ, γ_1). In particular, as our calculations show, P'_{0c} do not exist for $T_s \geq 0$.

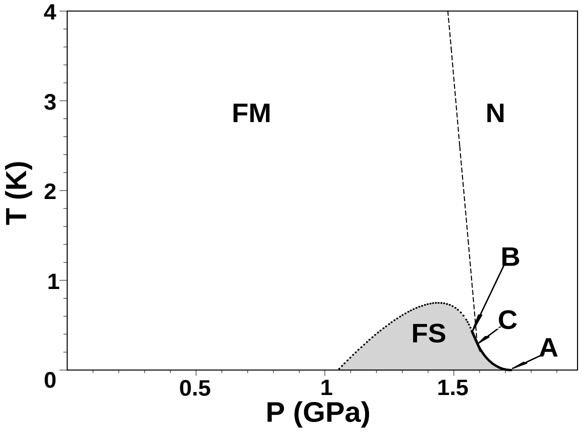

FIG. 5: Low-temperature part of the $T-P$ phase diagram of UGe$_2$, shown in Fig. 4. The points A, B, C are located in the high-pressure part ($P \sim P_c \sim 1.6$ GPa). The FS phase domain is shaded. The thick solid lines AC and BC show the first-order transitions N-FS, and FM-FS, respectively. Other notations are explained in Figs. 1, 2.

The analytical calculation of the critical pressures P_{0c} and P'_{0c} for the general case of $T_s \neq 0$ leads to very complex conditions for the appearance of second critical field P'_{0c}. The correct treatment for $T_s \neq 0$ can be performed within the two-domain picture of the phase FS. The complete study of this case is beyond our aims, but here we will illustrate our arguments by investigation of the conditions, under which the critical pressure P_{oc} occurs in systems with $T_s \approx 0$. Moreover, we will present the general result for $P_{0c} \geq 0$ and $P'_{0c} \geq 0$ in systems where $T_s \neq 0$.

Setting $T_{FS}(P_{0c}) = 0$ in Eq. (12) we obtain the following quadratic equation

$$\tilde{\gamma}_1 m_{0c}^2 - \tilde{\gamma} m_{0c} - \tilde{T}_s = 0 \qquad (15)$$

for the reduced magnetization

$$m_{0c} = [-t(0, \tilde{P}_{oc})]^{1/2} = (1 - \tilde{P}_{0c})^{1/2} \qquad (16)$$

and, hence, for $\tilde{P}_{0c}$. For $T_s \neq 0$ the Eqs. (15) and (16) have two solutions with respect to $\tilde{P}_{0c}$. For some sets of material parameters these solutions satisfy the physical requirements for P_{0c} and P'_{0c} and can be identified with the critical pressures. The conditions for existence of P_{0c} and P'_{0c} can be obtained either by analytical calculations, or by numerical analysis for particular values of the material parameters.

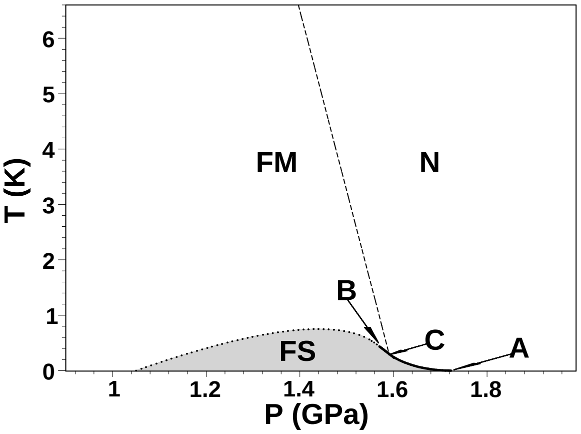

FIG. 6: High-pressure part of the phase diagram of UGe$_2$, shown in Fig. 4. Notations are explained in Figs. 1, 2, 4, 5.

For $T_s = 0$, the trivial solution $\tilde{P}_{0c} = 1$ corresponds to $P_{0c} = P_0 > P_B$ and, hence, does not satisfy the physical requirements. The second solution

$$\tilde{P}_{0c} = 1 - \frac{\tilde{\gamma}^2}{\tilde{\gamma}_1^2} \qquad (17)$$

is positive for

$$\frac{\gamma_1}{\gamma} \geq 1 \qquad (18)$$

and, as shown below, it gives the location of the quantum critical point ($T = 0, P_{0c} < P_m$). At this quantum critical point, the equilibrium magnetization m_{0c} is described by $m_{0c} = \gamma/\gamma_1$ and is twice bigger that the magnetization $m_m = \gamma/2\gamma_1$ [22] at the maximum of the curve $T_{FS}(P)$.

By taking $\tilde{P}_m$ from Table 1, we can show that the solution (17) satisfies the condition $P_{0c} < \tilde{P}_m$ for $n = 1$, if

$$\gamma_1 < 3\kappa \qquad (19)$$

and for $n = 2$ (SFT case), when

$$\gamma < 2\sqrt{3}\kappa. \qquad (20)$$

Finally, we determine the conditions under which the maximum T_m of the curve $T_{FS}(P)$ occurs at non-negative pressures. For $n = 1$, we obtain that $P_m \geq 0$ for $n = 1$, if

$$\frac{\gamma_1}{\gamma} \geq \frac{1}{2}\left(1 + \frac{\gamma_1}{\kappa}\right)^{1/2}, \qquad (21)$$

whereas for $n = 2$, the condition is

$$\frac{\gamma_1}{\gamma} \geq \frac{1}{2}\left(1 + \frac{\gamma^2}{4\kappa^2}\right)^{1/2}. \qquad (22)$$

Obviously, the conditions (18)-(22) are compatible with one another. The condition (21) is weaker than the condition (18), provided the inequality (19) is satisfied. The same is valid for the condition (22), if the inequality (20) is valid. In Sec. IV we will show that these theoretical predictions are confirmed by the experimental data.

Doing in the same way the analysis of Eq. (12) some results may easily be obtained for $T_s \neq 0$. In this more general case the Eq. (12) has two nontrivial solutions that yield two possible values of the critical pressure.

$$\tilde{P}_{0c(\pm)} = 1 - \frac{\gamma^2}{4\gamma_1^2}\left[1 \pm \left(1 + \frac{4\tilde{T}_s\kappa\gamma_1}{\gamma^2}\right)^{1/2}\right]^2. \qquad (23)$$

The relation $\tilde{P}_{0c(-)} \geq \tilde{P}_{0c(+)}$ is always true. Therefore, to have both $\tilde{P}_{0c(\pm)} \geq 0$, it is enough to require that $\tilde{P}_{0c(+)} \geq 0$. Having in mind that for the phase diagram shape, we study, $\tilde{T}_m > 0$, and according to the result for $\tilde{T}_m$ in Table 1, this leads to inequality $\tilde{T}_s > -\gamma^2/4\kappa\gamma_1$. So, we obtain that $\tilde{P}_{0c(+)} \geq 0$ will exist, if

$$\frac{\gamma_1}{\gamma} \geq 1 + \frac{\kappa\tilde{T}_s}{\gamma}, \qquad (24)$$

which generalizes the condition (18).

Now we can identify the pressure $P_{0c(+)}$ with the lower critical pressure P_{0c}, and $P_{0c(-)}$ with the upper critical pressure P'_{0c}. Therefore, for wide variations of the material parameters, the theory (1) describes a quantum critical point P_{oc} that exists, provided the condition (24) is satisfied. The quantum critical point ($T = 0, P_{0c}$) exists in UGe$_2$ and, perhaps, in other p-wave ferromagnetic superconductors, for example, in UIr.

Our results predict the appearance of second critical pressure - the upper critical pressure P'_{oc} that exists under more restricted conditions and, hence, can be observed for those systems, where $T_s < 0$. As mentioned in Sec. III.B, for very extreme negative values of T_s, when $T_B < 0$, the upper critical pressure $P'_{0c} > 0$ occurs, whereas the lower critical pressure $P_{0c} > 0$ does not appear. But especially this situation should be investigated in a different way, namely, one should keep $T_{FS}(0)$ different from zero in Eq. (12), and consider a form of the FS phase domain in which the curve $T_{FS}(P)$ terminates at $T = 0$ for $P'_{0c} > 0$, irrespective of whether the maximum T_m exists or not. In such geometry of the FS phase domain, the maximum $T_(P_m)$ may exist only in quite unusual cases, if it exists at all.

The quantum and thermal fluctuation phenomena in the vicinities of the two critical pressures P_{0c} and P'_{0c} need a non-standard RG treatment because they are related with the fluctuation behavior of the superconducting field $\boldsymbol{\psi}$ far below the ferromagnetic phase transitions, where the magnetization $\boldsymbol{M}$ does not undergo significant fluctuations and can be considered uniform. The presence of uniform magnetization produces couplings of $\boldsymbol{M}$

and $\boldsymbol{\psi}$ which are not present in previous RG studies and need a special analysis.

IV. APPLICATION TO METALLIC COMPOUNDS

A. Theoretical outline of the phase diagram

In order to apply the above displayed theoretic calculations, following from the free energy (2), for the outline of $T-P$ diagram of any material, we need information about the values of P_0, T_{f0}, T_s, κ γ, and γ_1. The temperature T_{f0} can be obtained directly from the experimental phase diagrams. The pressure P_0 is either identical or very close to the critical pressure P_c, for which the N-FM phase transition line terminates at $T\sim 0$. The temperature T_s of the generic superconducting transition is not available from the experiments because, as mentioned above pure superconducting phase not coexisting with ferromagnetism has been not observed. This can be considered as an indication that T_s is small and does not produce a measurable effect. So the generic superconducting temperature will be estimated on the basis of following general arguments. For $T_f(P) > T_s$ we must have $T_s(P) = 0$ at $P \geq P_c$, where $T_f(P) \leq 0$ and for $0 \leq P \leq P_0$, $T_s < T_C$. Therefore for materials where T_C is too small to be observed experimentally, T_s can be ignored.

As far as the shape of FM-FS transition line is well described by Eq. (12) we will make use of additional data from available experimental phase diagram for ferromagnetic superconductors. For example, in ZrZn$_2$ these are the observed values of $T_{FS}(0)$ and the slope $\rho_0 \equiv [\partial T_{FS}(P)/\partial P]_0 = (T_{f0}/P_0)\tilde{\rho}_0$ at $P=0$. For UGe$_2$, where a maximum is observed on the phase transition line, we can use the experimental values for T_m, P_m, and also for P_{0c}. The interaction parameters $\tilde{\gamma}$ and $\tilde{\gamma}_1$ are derived using Eq. (12) and the expressions for $\tilde{T}_m$, $\tilde{P}_m$, and $\tilde{\rho}_0$, see Table 1. The parameter κ is chosen by fitting the expression for the critical-end point T_C.

B. Diagram of ZrZn$_2$

Experiments for ZrZn$_2$ [13] give the following values: $T_{f0} = 28.5$ K, $T_{FS}(0) = 0.29$ K, $P_0 \sim P_c = 21$ kbar. The curve $T_F(P) \sim T_f(P)$ is almost a straight line, which directly indicates that $n=1$ is adequate in this case for the description of the P-dependence. The slope for $T_{FS}(P)$ at $P=0$ is estimated from the condition that its magnitude should not exceed $T_{f0}/P_c \approx 0.014$ as we have assumed that the transition line is straight one, so in result we have $-0.014 < \rho \leq 0$. This ignores the presence of a maximum. The available experimental data for ZrZn$_2$, do not give clear indications whether a maximum at (T_m, P_m) exists. If there is a maximum at $P=0$ this will mean $\rho_0 = 0$, and a maximum with $T_m \sim T_{FS}(0)$ and $P_m \ll P_0$ will give $0 \leq \rho_0 < 0.005$. We may choose that $\rho_0 = 0$, then $\tilde{\gamma} \approx 0.02$ and $\tilde{\gamma}_1 \approx 0.01$, similar values for the parameters are obtained for any $|\rho_0| \leq 0.003$.

The multi-critical points A and C cannot be distinguished experimentally as the experimental accuracy [13] is less than ~ 25 mK in the high-pressure domain ($P \sim 20-21$ kbar). Having this mind we can propose as initial assumption that $T_C \sim 10$ mK, which corresponds to $\kappa \sim 10$, see Table 1. We have calculated the $T-P$ diagram using $\rho_0 = 0$ and $\rho_0 = 0.003$, as well as the other parameters, discussed above. The differences, obtained in these two cases, are negligible.

In Fig. 1 we show the phase diagram of ZrZn$_2$ calculated directly from the free energy (2) for $n=1$, the above mentioned values of T_s, P_0, T_{f0}, κ, and values of $\tilde{\gamma} \approx 0.2$ and $\tilde{\gamma}_1 \approx 0.1$ which ensure $\rho_0 \approx 0$. The obtained coordinates of characteristic points are the following: $P_A \sim P_c = 21.42$ kbar, $T_A = T_F(P_c) = T_{FS}(P_c) = 0$ K; $P_B = 20.79$ kbar, $T_B = 0.0495$ K, and $P_C = 20.98$ kbar, $T_C = 0.0259$ K .

In Fig. 2, the low-T region is seen in more detail with A, B, C points, respectively. The dotted $T_{FS}(P)$ curve, represents the phase transition line FM-FS of second order and has a maximum $T_m = 0.290$ K at $P = 0.18$ kbar, which is slightly above $T_{FS}(0) = 0.285$ K. The straight solid line BC in Fig. 2 shows the first order FM-FS phase transition which occurs for $P_B < P < P_C$. The solid AC line shows the first order N-FS phase transition and the dashed line stands for the N-FM phase transition of second order.

Although the expanded temperature scale in Fig. 2, the difference $[T_m - T_{FS}(0)] = 5$ mK can hardly be seen. The calculations, both analytical and numerical, lead to the conclusion that if we want to locate the point *max* exactly at $P=0$ we have to take values of $\tilde{\gamma}$ and $\tilde{\gamma}_1$ with accuracy up to 10^{-4}. This may be considered as an indication that the *max* for parameters corresponding to ZrZn$_2$ is very sensitive to very small changes of parameters $\tilde{\gamma}$ and $\tilde{\gamma}_1$ around the values 0.2 and 0.1, respectively. Our initial idea was to present a diagram with $T_m = T_{FS}(0) = 0.29$ K and $\rho_0 = 0$, with the point of maximum being exactly at $P=0$, but the final phase diagram slightly departs from this picture because of the mentioned sensitivity of the result on the values of the interaction parameters γ and γ_1.

We have also calculated the theoretical phase diagram of ZrZn$_2$ for $\rho_0 = 0.003$ and initial values of $\tilde{\gamma}$ and $\tilde{\gamma}_1$ which differ from $\tilde{\gamma} = 2\tilde{\gamma}_1 = 0.2$ only by numbers of order $10^{-3} - 10^{-4}$ [26]. The obtained values for the coordinates of the maximum are: $T_m = 0.301$ K at $P_m = 6.915$ kbar. This result confirms the mentioned sensitivity of the location of the maximum T_m towards slight variations of the material parameters. Experimental investigations of this low temperature-low pressure region with higher accuracy may help to locate this maximum with better precision.

We show by Fig. 3 the high-pressure part of same phase diagram . As far as the experimental phase diagram [13] has restricted accuracy in this range of temperatures and pressures, it is important to draw the attention to the first order phase transitions, shown by solid lines BC (FM-FS) and AC (N-FS) as this interesting topology of the phase diagram of $ZrZn_2$ in the high-pressure domain ($P_B < P < P_A$) is not seen in the experiments. In fact the line AC is quite flat but not straight as the line BC. We hope that the detailed theoretical results for those parts of the phase diagram, where experimental data are lacking, may stimulate the further experiments in those ranges of pressure and temperature. The theoretical diagram, shown in Fig. 1, looks almost the same as the experimental one as far as there the details are smeared. Note, that the theoretical diagram is a direct result of calculations with the free energy (2) and the proposed P-dependence of its parameters, without any approximations and simplifying assumptions.

The theoretical phase diagram reflects well the main features of the experimental behavior [13], including the claimed change in the order of the FM-FS phase transition at relatively high P. Within the present model the N-FM transition is of second order up to $P_C \sim P_c$. Experiments give that the first order N-FM transition continues to much lower P values, and if this result is reliable, the theory can be easily modified to include this by a change of sign of b_f. Then a new tricritical point will appear, located at some $P_{tr} < P_C$ on the N-FM transition line. Since $T_C > 0$, a direct N-FS phase transition of first order is predicted in accord with conclusions from de Haas–van Alphen experiments [32] and some theoretical studies [33]. Such transition may not occur in other cases where $T_C = 0$. In spin-fluctuation theory($n = 2$) the diagram topology remains the same but points B and C are slightly shifted to higher P, typically by about $0.01 - 0.001$ kbar.

C. Diagram of UGe_2

The experimental data for UGe_2 give $T_{f0} = 52$ K, $P_c = 1.6$ GPa ($\equiv 16$ kbar), $T_m = 0.75$ K, $P_m \approx 1.15$ GPa, [2], and $P_{0c} \approx 1.05$ GPa [2, 3, 4, 5]. We use again $n = 1$ in the pressure dependence of $T_f(P)$ (4). From the above cited values for T_m and P_{0c} we obtain $\tilde{\gamma} \approx 0.0984$ and $\tilde{\gamma_1} \approx 0.1678$. The temperature $T_C \sim 0.1$ K corresponds to $\kappa \sim 4$.

In Fig. 4 we show the calculated with these initial parameters $T-P$ diagram of UGe_2. We have assumed that $T_s = 0$ in compliance with the arguments in Sec. III.A. The location of points A, B, C on the phase diagram is given by the following values: $T_A = 0$ K, $P_A = 1.723$ GPa, $T_B = 0.481$ K, $P_B = 1.563$ GPa, $T_C = 0.301$ K, and $P_C = 1.591$ GPa. Figs. 5 and 6 show the details of low-temperature and the high-pressure parts of this phase diagram, respectively.

Generally the main features of experimental curves are properly modelled by the theoretical T-P diagram of UGe_2, although there is some discrepancy in the numerical values for P_m corresponding to the maximum. Theoretically it is calculated as ~ 1.44 GPa in Fig. 4 which is about 0.3 GPa higher than found experimentally [4, 5]. If the experimental measurement are precise and give correct results for P_m, this difference may be attributed to the so-called (T_x) metamagnetic phase transition in UGe_2. It manifests in an abrupt change of the magnetization value in the vicinity of P_m. The possibility of metamagnetic transition is not considered in our model, but we may suppose that it will change the shape of $T_{FS}(P)$ making more symmetric the slope of curve around P_m and lowering it together with P_B and P_C. We have tried to obtain a lower P_m value, keeping T_m unchanged within the model (2), but this leads to a change of P_{c0} to a value that disagrees with experiment. In spin-fluctuation approach ($n = 2$) the multi-critical points are located at slightly higher P (by about 0.01 GPa), as for $ZrZn_2$. Therefore, the results from spin-fluctuation theory are slightly worse than the results obtained from the usual linear approximation ($n = 1$) for the parameter t.

In principle, the location of P_m both for $ZrZn_2$ and UGe_2 may be tuned better within the present model (1), if we take into account the anisotropy effects. Previous calculations [22] show that the inclusion, especially of spin-triplet Cooper pair anisotropy (the u_s-term in the Eq. (1)), changes the values of coordinates of points A, B, C and *max*. The problem is that the anisotropy in the present status of knowledge may serve only as a fitting parameter, because no proper information from microscopic theories is available both for its sign and magnitude. But such fitting from general considerations can obscure other effects, as the mentioned above metamagnetic transition in UGe_2, and even lead to some wrong interpretations when comparing the experimental and theoretical curves.

D. Two types of ferromagnetic superconductors with spin-triplet electron pairing

The estimates for UGe_2 give that $\gamma_1\kappa \approx 1.9$, so the condition for $T_{FS}(P)$ to have a maximum found from Eq. (12) is satisfied. As we have discussed for $ZrZn_2$, the location of this maximum can be hard to fix accurately in experiments. However, P_{c0} can be more easily distinguished, as in the UGe_2 case. Then we have a well-established quantum (zero-temperature) phase transition of second order, i.e., a quantum critical point at some critical pressure $P_{0c} \geq 0$. As shown in Sec. III.C, under special conditions the quantum critical points could be two: at the lower critical pressure $P_{0c} < P_m$ and the upper critical pressure $P'_{0c} < P_m$. This type of behavior in systems with $T_s = 0$ (as UGe_2) occurs when the criterion (18) is satisfied. Such systems (which we label as U-type) are essentially different from those such as $ZrZn_2$ where $\gamma_1 < \gamma$ and hence $T_{FS}(0) > 0$. In this latter case (Zr-type compounds), a maximum $T_m > 0$ may sometimes occur, as discussed earlier. We note that the ratio γ/γ_1 reflects a balance effect of two interactions between $\boldsymbol{\psi}$-$\boldsymbol{M}$. When the trigger interaction, represented by γ, prevails, the Zr-type behavior is found where superconductivity exists at $P = 0$. The same ratio can be expressed as $\gamma_0/\delta M_0$, which emphasizes that the ground state value of the magnetization at $P = 0$ is also relevant. Alternatively, one may refer to these two basic types of spin-triplet FSs as "type I" (for example, for the "Zr-type compounds"), and "type II" - for the U-type FS compounds.

As we see from this classification, the two types of spin-triplet ferromagnetic superconductors have quite different phase diagram topologies although some fragments have common features. The same classification can include systems with $T_s \neq 0$ but in this case one should use the more general criterion (24).

E. Other compounds

In URhGe, $T_f(0) \sim 9.5$ K and $T_{FS}(0) = 0.25$ K and, therefore, as in ZrZn$_2$,here the spin-triplet superconductivity appears at ambient pressure deeply in the ferromagnetic phase domain [6, 7, 8]. Although some similar structural and magnetic features with UGe$_2$ the results in Ref. [8] of measurements under high pressure show that, unlike the behavior of ZrZn$_2$ and UGe$_2$, the ferromagnetic phase transition temperature $T_F(P) \sim T_f(P)$ has a slow linear increase up to 140 kbar without any experimental indications that the N-FM transition line may change its behavior at higher pressures and show a negative slope in direction of low temperature up to a quantum critical point $T_F = 0$ at some critical pressure P_c. Such behavior of the generic ferromagnetic phase transition temperature cannot be explained by our initial assumption for the function $T_f(P)$ which was intended to explain phase diagrams where the ferromagnetic order is depressed by the pressure and vanishes at $T = 0$ for some critical pressure P_c. The $T_{FS}(P)$ line of URhGe shows a clear monotonic negative slope to $T = 0$ at pressures above 15 kbar and the extrapolation [8] of the experimental curve $T_{FS}(P)$ tends a quantum critical point $T_{FS}(P'_{oc}) = 0$ at $P_{0c} \sim 25 - 30$ kbar. Within the framework of the phenomenological theory (2), this $T - P$ phase diagram can be explained after a modification of $T_f(P)$-dependence is made, and by introducing a convenient nontrivial pressure dependence of the interaction parameter γ. Such modifications of the present theory are possible and follow from important physical requirements related with the behavior of the f-band electrons in URhGe. Unlike UGe$_2$, where the pressure increases the hybridization of the $5f$ electrons with band states leading to a suppression of the spontaneous magnetic moment M, in URhGe this effects is followed by a stronger effect of enhancement of the exchange coupling due to the same hybridization, and this effect leads to the slow but stable linear increase of the function $T_F(P)$ [8]. These effects should be taken into account in the modelling of the pressure dependence of the parameters of the theory (2)when applied to URhGe.

Another ambient pressure FS phase has been observed in experiments on UCoGe [9]. Here the experimentally derived slopes of the functions $T_F(P)$ and $T_{FS}(P)$ at relatively small pressures are opposite compared to those for URhGe and, hence, the $T - P$ phase diagram of this compound can be treated within the present theoretical scheme without substantial modifications.

Like in UGe$_2$, the FS phase in UIr [12] is embedded in the high-pressure/low-temperature part of the ferromagnetic phase domain near the critical pressure P_c which means that UIr is certainly a U-type compound (see Sec. IV.D). In UGe$_2$ there is one meta-magnetic phase transition between two ferromagnetic phases (FM1 and FM2), in UIr there are three ferromagnetic phases and the FS phase is located in the low-T/high-P domain of the third of them - the phase FM3. There are two meta-magnetic-like phase transitions: FM1-FM2 transition which is followed by a drastic decrease of the spontaneous magnetization when the lower-pressure phase FM1 transforms to FM2, and a peak of the ac susceptibility but lack of observable jump of the magnetization at the second (higher pressure) "meta-magnetic" phase transition from FM2 to FM3. Unlike the picture for UGe$_2$, in UIr both transitions, FM1-FM2 and FM2-FM3, are far from the maximum $T_m(P_m)$, so in this case one can hardly speculate that the *max* is produced by the nearby jump of magnetization. UIr seems to be a U-type spin-triplet ferromagnetic superconductor.

V. FINAL REMARKS

Finally, even in its simplified form, this theory has been shown to be capable of accounting for a wide variety of experimental behavior. A natural extension to the theory is to add a $\boldsymbol{M}^6$ term which provides a formalism to investigate possible meta-magnetic phase transitions [37] and extend some first order phase transition lines. Another modification of this theory, with regard to applications to other compounds, is to include a P dependence for some of the other GL parameters. The fluctuation and quantum correlation effects can be considered by the respective field-theoretical action of the system, where the order parameters $\boldsymbol{\psi}$ and $\boldsymbol{M}$ are not uniform but rather space and time dependent. The vortex (spatially non-uniform) phase due to the spontaneous magnetization $\boldsymbol{M}$ is another phenomenon which can be investigated by a generalization of the theory by considering non-uniform order parameters fields $\boldsymbol{\psi}$ and $\boldsymbol{M}$ (see, e.g., Ref. [38, 39]). Note, that such theoretical treatments are quite complex and require a number of approximations. As already noted in this paper the magnetic fluctuations stimulate first order phase transitions for both finite and zero phase transition temperatures.

ACKNOWLEDGEMENTS: The authors thank M. G. Cottam for useful discussions and A. Harada, and S. M. Hayden for valuable private communications. One of us (D.I.U.) thanks the University of Western Ontario for hospitality. Partial support from NFSR-Sofia (through grant Ph. 1507) is also acknowledged.

---

[1] D. Vollhardt and P. Wölfle, it The Superfluid Phases of Helium 3 (Taylor & Francis, London, 1990); D. I. Uzunov, in: *Advances in Theoretical Physics*, edited by E. Caianiello (World Scientific, Singapore, 1990), p. 96; M. Sigrist and K. Ueda, Rev. Mod. Phys. **63**, 239 (1991).

[2] S. S. Saxena, P. Agarwal, K. Ahilan, F. M. Grosche, R. K. W. Haselwimmer, M.J. Steiner, E. Pugh, I. R. Walker, S.R. Julian, P. Monthoux, G. G. Lonzarich, A. Huxley. I. Sheikin, D. Braithwaite, and J. Flouquet, Nature **406**, 587 (2000).

[3] A. Huxley, I. Sheikin, E. Ressouche, N. Kernavanois, D. Braithwaite, R. Calemczuk, and J. Flouquet, Phys. Rev. **B63**, 144519 (2001).

[4] N. Tateiwa, T. C. Kobayashi, K. Hanazono, A. Amaya, Y. Haga. R. Settai, and Y. Onuki, J. Phys. Condensed Matter **13**, L17 (2001).

[5] A. Harada, S. Kawasaki, H. Mukuda, Y. Kitaoka, Y. Haga, E. Yamamoto, Y. Onuki, K. M. Itoh, E. E. Haller, and H. harima, Phys. Rev. B **75**, 140502 (2007).

[6] D. Aoki, A. Huxley, E. Ressouche, D. Braithwaite, J. Flouquet, J-P.. Brison, E. Lhotel, and C. Paulsen, Nature **413**, 613 (2001).

[7] F. Hardy, A. Huxley, Phys. Rev. Lett. **94**, 247006 (2005).

[8] F. Hardy, A. Huxley, J. Flouquet, B. Salce, G. Knebel, D. Braithwate, D. Aoki, M. Uhlarz, and C. Pfleiderer, Physica B **359-361** 1111 (2005).

[9] N. T. Huy, A. Gasparini, D. E. de Nijs, Y. Huang, J. C. P. Klaasse, T. Gortenmulder, A. de Visser, A. Hamann, T. Görlach, and H. v. Löhneysen, Phys. Rev. Lett. **99**, 067006 (2007).

[10] N. T. Huy, D. E. de Nijs, Y. K. Huang, and A. de Visser, Phys. Rev. Lett. **100**, 077001 (2008).

[11] T. Akazawa, H. Hidaka, H. Kotegawa, T. C. Kobayashi, T. Fujiwara, E. Yamamoto, Y. Haga, R. Settai, and Y. Onuki, Physica B **359-361**, 1138 (2005).

[12] T. C. Kobayashi,S. Fukushima, H. Hidaka, H. Kotegawa, T. Akazawa, E. Yamamoto, Y. Haga, R. Settai, and Y. Onuki, Physica B **378-361**, 378 (2006).

[13] C. Pfleiderer, M. Uhlatz, S. M. Hayden, R. Vollmer, H. v. Löhneysen, N. R. Berhoeft, and G. G. Lonzarich, Nature **412**, 58 (2001).

[14] E. A. Yelland, S. J. C. Yates, O. Taylor, A. Griffiths, S. M. Hayden, and A. Carrington, Phys. Rev. B **72**, 184436 (2005).

[15] E. A. Yelland, S. M. Hayden, S. J. C. Yates, C. Pfleiderer, M. Uhlarz, R. Vollmer, H. v Löhneysen, N. R. Bernhoeft, R. P. Smith, S. S. Saxena, and N. Kimura, Phys. Rev. **B72**, 214523 (2005).

[16] C. J. Bolesh and T. Giamarchi, Phys. Rev. Lett. **71**, 024517 (2005); R. D. Duncan, C. Vaccarella, and C. A. S. de Melo, Phys. Rev. B **64**, 172503 (2001).

[17] A. H. Nevidomskyy, Phys. Rev. Lett. **94**, 097003 (2005).

[18] D. I. Uzunov, *Theory of Critical Phenomena* (World Scientific, Singapore, 1993).

[19] K. Machida and T. Ohmi, Phys. Rev. Lett. **86**, 850 (2001).

[20] M. B. Walker and K. V. Samokhin, Phys. Rev. Lett. **88**, 207001 (2002); K. V. Samokhin and M. B. Walker, Phys. Rev. B **66**, 024512 (2002); Phys. Rev. B **66**, 174501 (2002).

[21] J. Linder, A. Sudbo, Phys. Rev. B **76**, 054511 (2007); J. Linder, I. B. Sperstad, A. H. Nevidomskyy, M. Cuoco, and A. Sodbo, Phys. Rev. **77**, 184511 (2008); J. Linder, T. Yokoyama, and A. Sudbo, Phys. Rev. B **78**, 064520 (2008); J. Linder, A. H. Nevidomskyy, A. Sudbo, Phys. Rev. B **78**, 172502 (2008).

[22] D. V. Shopova and D. I. Uzunov, Phys. Rev. **72**, 024531 (2005); Phys. Lett. A **313**, 139 (2003).

[23] D. V. Shopova and D. I. Uzunov, in: *Progress in Ferromagnetism Research*, ed. by V. N. Murray (Nova Science Publishers, New York, 2006), p. 223; D. V. Shopova and D. I. Uzunov, J. Phys. Studies , **4**, 426 (2003) 426; D. V. Shopova and D. I. Uzunov, Compt. Rend Acad. Bulg. Sci. **56**, 35 (2003) 35; D. V. Shopova, T. E. Tsvetkov, and D. I. Uzunov, Cond. Matter Phys. **8**, 181 (2005) 181; D. V. Shopova, and D. I. Uzunov, Bulg. J. of Phys. **32**, 81 (2005).

[24] R. A. Cowley, Adv. Phys. **29**, 1 (1980); J-C. Tolédano and P. Tolédano, *The Landau Theory of Phase Transitions* (World Scientific, Singapore, 1987).

[25] K. K. Murata and S. Doniach, Phys. Rev. Lett. **29**, 285 (1972); G. G. Lonzarich and L. Taillefer, J. Phys. C: Solid State Phys. **18**, 4339 (1985); T. Moriya, J. Phys. Soc. Japan **55**, 357 (1986); H. Yamada, Phys. Rev. B **47**, 11211 (1993).

[26] M. G. Cottam, D. V. Shopova and D. I. Uzunov, Phys. Lett. A (2008), in press.

[27] D. V. Shopova and D. I. Uzunov, Phys. Rep. C **379**, 1 (2003).

[28] E. P. Wohlfarth, J. Appl. Phys. **39**, 1061 (1968); Physica B&C **91B**, 305 (1977).

[29] P. Misra, *Heavy-Fermion Systems*, (Elsevier, Amsterdam, 2008).

[30] K. G. Sandeman, G. G. Lonzarich, and A. J. Schofield, Phys. Rev. Lett. **90**, 167005 (2003).

[31] T. F. Smith, J. A. Mydosh, and E. P. Wohlfarth, Phys. rev. Lett. **27**, 1732 (1971); G. Oomi, T. Kagayama, K. Nishimura, S. W. Yun, and Y. Onuki, Physica B **206**, 515 (1995).

[32] N. Kimura *et al.*, Phys. Rev. Lett. **92** , 197002 (2004).

[33] M. Uhlarz, C. Pfleiderer, and S. M. Hayden, Phys. Rev. Lett. **93**, 256404 (2004).

[34] D. I. Uzunov, Phys. Rev. **B74**, 134514 (2006); Europhys. Lett. **77**, 20008 (2007).

[35] D. Belitz, T. R. Kirkpatrick, J. Rollbühler, Phys. Rev. Lett. **94**, 247205 (2005); G. A. Gehring, Europhys. Lett. **82**, 60004 (2008).

[36] B. I. Halperin, T. C. Lubensky, and S. K. Ma, Phys. Rev. Lett. **32**, 292 (1974); J-H. Chen, T. C. Lubensky, and D. R. Nelson, *Phys. Rev.* **B17**, 4274 (1978).

[37] A. Huxley, I. Sheikin, and D. Braithwaite, Physica **B 284-288**, 1277 (2000).

[38] S Tewari, D. Belitz, T. R. Kirkpatrick, and J. Toner, Phys. Rev. Lett. **93**, 177002 (2004).
[39] Q. Li, D. Belitz, and T. R. Kirkpatrick, Phys. Rev. B **74**, 134505 (2006).